

A solution method for decomposing vector fields in Hamilton energy

Xin Zhao(赵昕), Ming Yi(易鸣), Zhou-Chao Wei(魏周超), Yuan Zhu(朱媛), and Lu-Lu Lu(鹿露露)

Citation: Chin. Phys. B, 2024, 33 (**9**): 098702. DOI: 10.1088/1674-1056/ad5a74
Journal homepage: http://cpb.iphy.ac.cn; http://iopscience.iop.org/cpb

What follows is a list of articles you may be interested in

A progressive surrogate gradient learning for memristive spiking neural network

Shu Wang(王姝), Tao Chen(陈涛), Yu Gong(龚钰), Fan Sun(孙帆), Si-Yuan Shen(申思远), Shu-Kai Duan(段书凯), and Li-Dan Wang(王丽丹)

Chin. Phys. B, 2023, 32 (**6**): 068704. DOI: 10.1088/1674-1056/acb9f6

Simulation of the physical process of neural electromagnetic signal generation based on a simple but functional bionic Na^+ channel

Fan Wang(王帆), Jingjing Xu(徐晶晶), Yanbin Ge(葛彦斌), Shengyong Xu(许胜勇),Yanjun Fu(付琰军), Caiyu Shi(石蔡语), and Jianming Xue(薛建明)

Chin. Phys. B, 2022, 31 (**6**): 068701. DOI: 10.1088/1674-1056/ac3cac

Dynamics and coherence resonance in a thermosensitive neuron driven by photocurrent

Ying Xu(徐莹), Minghua Liu(刘明华), Zhigang Zhu(朱志刚), Jun Ma(马军)

Chin. Phys. B, 2020, 29 (**9**): 098704. DOI: 10.1088/1674-1056/ab9dee

Cooperative impulsive formation control for networked uncertain Euler-Lagrange systems with communication delays

Liang-ming Chen(陈亮名), Chuan-jiang Li(李传江), Yan-chao Sun(孙延超), Guang-fu Ma(马广富)

Chin. Phys. B, 2017, 26 (**6**): 068703. DOI: 10.1088/1674-1056/26/6/068703

Energy dependence on the electric activities of a neuron

Song Xin-Lin (宋欣林), Jin Wu-Yin (靳伍银), Ma Jun (马军)

Chin. Phys. B, 2015, 24 (**12**): 128710. DOI: 10.1088/1674-1056/24/12/128710

A solution method for decomposing vector fields in Hamilton energy

Xin Zhao(赵昕), Ming Yi(易鸣), Zhou-Chao Wei(魏周超), Yuan Zhu(朱媛), and Lu-Lu Lu(鹿露露)†

School of Mathematics and Physics, China University of Geosciences, Wuhan 430074, *China*

(Received 13 May 2024; revised manuscript received 14 June 2024; accepted manuscript online 21 June 2024)

Hamilton energy, which reflects the energy variation of systems, is one of the crucial instruments used to analyze the characteristics of dynamical systems. Here we propose a method to deduce Hamilton energy based on the existing systems. This derivation process consists of three steps: step 1, decomposing the vector field; step 2, solving the Hamilton energy function; and step 3, verifying uniqueness. In order to easily choose an appropriate decomposition method, we propose a classification criterion based on the form of system state variables, i.e., type-I vector fields that can be directly decomposed and type-Ⅱ vector fields decomposed via exterior differentiation. Moreover, exterior differentiation is used to represent the curl of low-high dimension vector fields in the process of decomposition. Finally, we exemplify the Hamilton energy function of six classical systems and analyze the relationship between Hamilton energy and dynamic behavior. This solution provides a new approach for deducing the Hamilton energy function, especially in high-dimensional systems.

Keywords: Hamilton energy, dynamical systems, vector field, exterior differentiation

PACS: 87.19.L–, 87.19.Lj, 05.45.–a, 05.45.Pq **DOI:** 10.1088/1674-1056/ad5a74

1. Introduction

Hamilton energy is a crucial quantitative profiler that is frequently used in research of system dynamic behavior, including chaos synchronization and control of orbits. An appropriate energy function can help us measure the energy dissipation and production of the dynamic system reasonably.

In recent decades, the most common application of Hamilton energy has been to record the energy changes in a dynamic system of neurons after external stimuli.[1–3] The cognitive activity of the brain is accompanied by rich firing modes of neurons,[4] such as working memory and information processing in the central nervous system,[5] and changes of firing mode are often related to the energy levels of neurons.[6] The average energy consumption of the Hindmarsh–Rose (HR) neuron model was calculated at various external current values, and it was discovered that energy consumption of the neuron during signaling activity is particularly sensitive to the different firing regimes.[7]

In addition, temperature is also an important variable in the dynamic system. The regular conduct of biological physiological activities is directly impacted by temperature, and there is often an appropriate temperature range to optimum energy efficiency.[8] The effect of temperature on the firing pattern of neurons was investigated on a modified FitzHugh–Nagumo model. The results show that the dynamic behavior of neurons changes with the increase of temperature, and the Hamilton energy appears in ordered distribution under the temperature spatial gradient distribution.[9] Also covered was the relationship between temperature-sensitive Chay neurons' various burst kinetics and energy efficiency.[10] Analogously, the energy function of the HR neuron model can determine the values of the coupling intensity that might maximize the ratio of mutual information to energy consumption,[11] there by finding the appropriate coupling strength for interneuronal communication through this discovery. The communication between neurons is significantly impacted by the field coupling intensity in the four-variable HR model, which takes into account the electromagnetic field created by continuous ion transport across membranes.[12]

The storage and release of neuron energy can also be detected by energy function,[13] and it has been observed that the bursting and chaotic states may aid in the rapid release of energy within the neuron.[14] The patterns of energy dissipation of five classical systems were compared using the Hamilton energy function.[15] The Hamilton energy function of chaotic systems with different types of attractors was determined, and energy modulation was used to control the chaotic behaviors of these systems.[16] Another fascinating field of research involves the qualitative analysis of dynamical systems through observing the behavior of the energy function in phase space.[17] Through a phase diagram and energy analysis, Huang *et al.*[18] observed the coexistence of different energy orbits and equal energy orbits in a five-dimensional Hamiltonian conservative hyperchaotic system.

It is frequently discovered that the Hamilton energy is connected to other indications. For instance, in a fractal process, the energy of a multi-wing chaotic system is negatively correlated with its number of wings,[19] and when examining the dynamical behavior of a five-dimension HR neuronal model, it is discovered that the system's Hamilton energy

†Corresponding author. E-mail: lululu@cug.edu.cn

© 2024 Chinese Physical Society and IOP Publishing Ltd

function and the Lyapunov function have a similar role,[20] etc.

Hamilton energy plays a vital role in dynamical systems. Unfortunately, it is hard to find a general method to deduce the Hamilton energy function. In this work we find some common rules that different systems follow in different decomposition processes, and divide the systems into types I and Ⅱ based on the form of state variables. Therefore, based on the Helmholtz theorem, a solution method for decomposing vector fields in Hamilton energy is developed, and this method is still applicable to high-dimensional systems.

The rest of this paper is organized as follows: In Section 2, we describe the solution method and steps for solving the Hamilton energy function and point out the differences in the solution processes of different types of systems. In Section 3, the time evolution of Hamilton energy for six classical systems is calculated. In particular, we also investigate the dependence of average energy of the HR neuronal system and four-dimensional (4D) HR system receiving external forcing current on the amplitude and the angular frequency. Lastly, the summary and potential applications are provided in Section 4.

2. Theoretical description and solution method

A solution method was proposed to deduce the Hamilton energy function of systems: step 1, decomposition of the vector field; step 2, solving the energy function according to the equation; and step 3, verifying the uniqueness.

Step 1: Decomposing the vector field According to the Helmholtz theorem,[21] if the divergence, curl, and boundary conditions of a vector field $F(X)$ in space region V are known, the vector field in space region can be identified uniquely and can be expressed as a superposition of a vector field without divergence (conservative field) $f_{\rm c}(X)$ and a vector field without curl (gradient field) $f_{\rm d}(X)$, that is, $F(X)=f_{\rm c}(X)+f_{\rm d}(X)$. The conservative field $f_{\rm c}(X)$ contains the curl of the whole system, and the gradient field $f_{\rm d}(X)$ contains the divergence of the whole system. The theorem shows that any vector field consists of two parts: one is a vector field without divergence excited by a vortex source, and the other is a vector field without curl excited by the flux source, so only the flux source and the vortex source can lead to generation of the vector field, there are no other types of sources.

Type I: Directly decomposable vector fields Firstly, all the terms related to divergence in the system need to be put into the gradient field according to the divergence formula $\nabla\cdot F=(e_x\frac{\partial}{\partial x},e_y\frac{\partial}{\partial y},e_z\frac{\partial}{\partial z})\cdot(e_xF_x,e_yF_y,e_zF_z)$, and all the remaining terms remain in the vector field without divergence. Meanwhile, the terms containing divergence will not appear in field $f_{\rm c}(X)$. Finally, the constant terms can be set based on the research purpose and previous conventions. Generally speaking, after these steps, the terms related to curl and divergence will be completely decomposed and are located in $f_{\rm c}(X)$ and $f_{\rm d}(X)$, respectively.

There are many systems that can directly decompose vector fields, e.g., (I) Lorenz system:[22]

$$\begin{bmatrix}\dot{x}\\ \dot{y}\\ \dot{z}\end{bmatrix}=\begin{bmatrix}\sigma y-\sigma x\\ \rho x-y-xz\\ xy-\beta z\end{bmatrix}=\begin{bmatrix}\sigma y\\ \rho x-xz\\ xy\end{bmatrix}+\begin{bmatrix}-\sigma x\\ -y\\ -\beta z\end{bmatrix},$$

(Ⅱ) Chua system:[22]

$$\begin{bmatrix}\dot{x}\\ \dot{y}\\ \dot{z}\end{bmatrix}=\begin{bmatrix}\alpha y-\alpha x^3-\alpha cx\\ x+z-y\\ -\beta y\end{bmatrix}=\begin{bmatrix}\alpha y\\ x+z\\ -\beta y\end{bmatrix}+\begin{bmatrix}-\alpha x^3-\alpha cx\\ -y\\ 0\end{bmatrix},$$

(Ⅲ) Chen system:[15]

$$\begin{bmatrix}\dot{x}\\ \dot{y}\\ \dot{z}\end{bmatrix}=\begin{bmatrix}ay-ax\\ (c-a)x+cy-xz\\ xy-bz\end{bmatrix}=\begin{bmatrix}ay\\ (c-a)x-xz\\ xy\end{bmatrix}+\begin{bmatrix}-\alpha x\\ cy\\ -bz\end{bmatrix},$$

(Ⅳ) Lü–Chen (Lü) system:[15]

$$\begin{bmatrix}\dot{x}\\ \dot{y}\\ \dot{z}\end{bmatrix}=\begin{bmatrix}ay-ax\\ cy-xz\\ xy-bz\end{bmatrix}=\begin{bmatrix}ay\\ -xz\\ xy\end{bmatrix}+\begin{bmatrix}-ax\\ cy\\ -bz\end{bmatrix},$$

(Ⅴ) HR system:[7]

$$\begin{aligned}\begin{bmatrix}\dot{x}\\ \dot{y}\\ \dot{z}\end{bmatrix}&=\begin{bmatrix}y-\alpha x^3+bx^2+I_{\rm ext}-z\\ c-dx^2-y\\ r[s(x-x_0)-z]\end{bmatrix}\\&=\begin{bmatrix}y-z\\ -dx^2\\ rsx\end{bmatrix}+\begin{bmatrix}-\alpha x^3+bx^2+I_{\rm ext}\\ c-y\\ -rsx_0-rz\end{bmatrix},\end{aligned}$$

(Ⅵ) the 4D HR model:[11]

$$\begin{aligned}\begin{bmatrix}\dot{x}\\ \dot{y}\\ \dot{z}\\ \dot{\omega}\end{bmatrix}&=\begin{bmatrix}ay+bx^2-cx^3-dz+\xi I\\ e-fx^2-y-g\omega\\ m[-z+s(x+h)]\\ n[-k\omega+r(y+l)]\end{bmatrix}\\&=\begin{bmatrix}ay-dz\\ -fx^2-g\omega\\ msx\\ nry\end{bmatrix}+\begin{bmatrix}bx^2-cx^3+\xi I\\ e-y\\ msh-mz\\ nrl-nk\omega\end{bmatrix},\end{aligned}$$

(Ⅶ) the unified Lorenz system:[17]

$$\begin{aligned}\begin{bmatrix}\dot{x}\\ \dot{y}\\ \dot{z}\end{bmatrix}&=\begin{bmatrix}(25\alpha+10)(y-x)\\ (28-35\alpha)x+(29\alpha-1)y-xz\\ xy-\frac{\alpha+8}{3}z\end{bmatrix}\\&=\begin{bmatrix}(25\alpha+10)y\\ (28-35\alpha)x-xz\\ xy\end{bmatrix}+\begin{bmatrix}-(25\alpha+10)x\\ (29\alpha-1)y\\ -\frac{\alpha+8}{3}z\end{bmatrix},\end{aligned}$$

(Ⅷ) the generalized Lorenz system:[23]

$$\begin{bmatrix}\dot{x}\\ \dot{y}\\ \dot{z}\end{bmatrix}=\begin{bmatrix}-a(x-y)-byz\\ cx-y-xz\\ xy-dz\end{bmatrix}=\begin{bmatrix}ay-byz\\ cx-xz\\ xy\end{bmatrix}+\begin{bmatrix}-ax\\ -y\\ -dz\end{bmatrix},$$

(IX) the B–G system:[24]

$$\begin{bmatrix}\dot{x}\\ \dot{p}\\ \dot{q}\end{bmatrix} = \begin{bmatrix}\omega x-\frac{1}{2}(p+N)\\ -(\mu+b)p+(\mu-a-x)q-(\mu-b)N\\ -(\mu-a-x)p-(\mu+b)q+(u+a+x)N\end{bmatrix} = \begin{bmatrix}-\frac{1}{2}(p+N)\\ (\mu-a-x)q\\ -(\mu-a-x)p\end{bmatrix} + \begin{bmatrix}\omega x\\ -(\mu+b)p-(\mu-b)N\\ -(\mu+b)q+(u+a+x)N\end{bmatrix}.$$

In addition to the above-listed systems, there are many other systems that can be decomposed in this way.[25–28]

Type II: Vector fields decomposed by exterior differentiation However, some systems fail to follow the decomposition procedure mentioned above. After putting the term containing divergence into $f_{\rm d}(X)$, the curl of $f_{\rm d}(X)$ will not be zero, so it is necessary to recheck the curl of $f_{\rm d}(X)$.

Here is a method for checking the curl of a vector field: exterior differentiation. For the exterior differentiation operator d, it satisfies the following conditions: (1) It is a linear operator. (2) It becomes 0 after two actions, namely, $\mathrm{d}^2=0$. (3) 0-form: function $f(x,y,z)$ or $f(u,v)$; 1-form: external differential of 0-form, namely,

$$\mathrm{d}f(u,v)=\frac{\partial f}{\partial u}\mathrm{d}u+\frac{\partial f}{\partial v}\mathrm{d}v,$$

or

$$\mathrm{d}f(x,y,z)=\frac{\partial f}{\partial x}\mathrm{d}x+\frac{\partial f}{\partial y}\mathrm{d}y+\frac{\partial f}{\partial z}\mathrm{d}z. \tag{1}$$

There is a 1-form $f(x,y,z)=f_x(x,y,z)\mathrm{d}x+f_y(x,y,z)\mathrm{d}y+f_z(x,y,z)\mathrm{d}z$, and its 2-form can be computed as

$$\begin{aligned}\mathrm{d}f(x,y,z)&=\mathrm{d}[f_x(x,y,z)\mathrm{d}x]+\mathrm{d}[f_y(x,y,z)\mathrm{d}y]+\mathrm{d}[f_z(x,y,z)\mathrm{d}z]\\&=\Big(\frac{\partial f_x}{\partial x}\mathrm{d}x+\frac{\partial f_x}{\partial y}\mathrm{d}y+\frac{\partial f_x}{\partial z}\mathrm{d}z\Big)\mathrm{d}x\\&\quad+\Big(\frac{\partial f_y}{\partial x}\mathrm{d}x+\frac{\partial f_y}{\partial y}\mathrm{d}y+\frac{\partial f_y}{\partial z}\mathrm{d}z\Big)\mathrm{d}y\\&\quad+\Big(\frac{\partial f_z}{\partial x}\mathrm{d}x+\frac{\partial f_z}{\partial y}\mathrm{d}y+\frac{\partial f_z}{\partial z}\mathrm{d}z\Big)\mathrm{d}z\\&=\frac{\partial f_x}{\partial y}\mathrm{d}y\wedge\mathrm{d}x+\frac{\partial f_x}{\partial z}\mathrm{d}z\wedge\mathrm{d}x+\frac{\partial f_y}{\partial x}\mathrm{d}x\wedge\mathrm{d}y\\&\quad+\frac{\partial f_y}{\partial z}\mathrm{d}z\wedge\mathrm{d}y+\frac{\partial f_z}{\partial x}\mathrm{d}x\wedge\mathrm{d}z+\frac{\partial f_z}{\partial y}\mathrm{d}y\wedge\mathrm{d}z\\&=\Big(\frac{\partial f_z}{\partial y}-\frac{\partial f_y}{\partial z}\Big)\mathrm{d}y\wedge\mathrm{d}z+\Big(\frac{\partial f_x}{\partial z}-\frac{\partial f_z}{\partial x}\Big)\mathrm{d}z\wedge\mathrm{d}x\\&\quad+\Big(\frac{\partial f_y}{\partial x}-\frac{\partial f_x}{\partial y}\Big)\mathrm{d}x\wedge\mathrm{d}y.\end{aligned} \tag{2}$$

Then the curl of 1-form is the coefficient in front of 2-form.

By checking the curl of the gradient field, the Rössler system[22] has the above situation and needs to match $f_{\rm d}(X)$. (I) The Rössler system is

$$\begin{aligned}&\dot{x}=-y-z,\quad \dot{y}=x+ay,\\&\dot{z}=b+(x-c)z.\end{aligned} \tag{3}$$

According to the Helmholtz theorem and the decomposition method mentioned above, we first put the terms related to divergence in the gradient field according to the divergence calculation formula $\nabla\cdot f_{\rm c}(X)$, and the remaining terms in the vector field without divergence. We can get

$$f_{\rm c}=\begin{pmatrix}-y-z\\ x\\ b\end{pmatrix},\quad f_{\rm d}=\begin{pmatrix}0\\ ay\\ (x-c)z\end{pmatrix}. \tag{4}$$

We check the curl of the gradient field, assuming the 1-form to be

$$f=0\mathrm{d}x+ay\mathrm{d}y+[(x-c)z]\mathrm{d}z \tag{5}$$

and 2-form as

$$\begin{aligned}\mathrm{d}f&=\mathrm{d}[0\mathrm{d}x]+\mathrm{d}[ay\mathrm{d}y]+\mathrm{d}[(x-c)z\mathrm{d}z]\\&=(0\mathrm{d}x+0\mathrm{d}y+0\mathrm{d}z)\mathrm{d}x+(0\mathrm{d}x+a\mathrm{d}y+0\mathrm{d}z)\mathrm{d}y\\&\quad+[z\mathrm{d}x+0\mathrm{d}y+(x-c)\mathrm{d}z]\mathrm{d}z\\&=z\mathrm{d}z\wedge\mathrm{d}x.\end{aligned} \tag{6}$$

After calculation, the curl of $f_{\rm d}(X)$ is obviously nonzero, so we need to match it. Therefore, we complement $\frac{1}{2}z^2$ on the first element, and we need to add its opposite on the first element. Therefore, we can obtain

$$f_{\rm c}=\begin{pmatrix}-y-z-\frac{1}{2}z^2\\ x\\ b\end{pmatrix},\quad f_{\rm d}=\begin{pmatrix}\frac{1}{2}z^2\\ ay\\ (x-c)z\end{pmatrix}. \tag{7}$$

At this time, the Helmholtz decomposition theorem can be followed for $\mathrm{div}f_{\rm c}(X)=0$ and $\mathrm{rot}f_{\rm d}(X)=0$, and then the energy function can be calculated using the $f_{\rm d}(X)$ matched one. In addition, we find that this situation also occurs in other systems that require Helmholtz decomposition after matching the gradient field, e.g., (II) the motion equations of unconstrained particles:[29]

$$\begin{bmatrix}\dot{x}\\ \dot{x}_1\\ \dot{y}\\ \dot{y}_1\end{bmatrix}=\begin{bmatrix}x_1\\ ax-bx^2-cx_1y\\ y_1\\ ay-by^2-cxy_1\end{bmatrix}=\begin{bmatrix}x_1+\frac{1}{2}cy_1^2\\ ax-bx^2\\ y_1+\frac{1}{2}cx_1^2\\ ay-by^2\end{bmatrix}+\begin{bmatrix}-\frac{1}{2}cy_1^2\\ -cx_1y\\ -\frac{1}{2}cx_1^2\\ -cxy_1\end{bmatrix},$$

(III) the four-wing chaotic system:[30]

$$\begin{aligned}\begin{bmatrix}\dot{u}\\ \dot{v}\\ \dot{w}\end{bmatrix}&=\begin{bmatrix}\alpha w-8uv\\ 11u^2+3v^2+w^2+\beta uw-3c^2\\ -\alpha u+2(1-b)vw-\beta uv\end{bmatrix}\\&=\begin{bmatrix}\alpha w\\ 11u^2+w^2+\beta uw-(1-b)w^2+4u^2\\ -\alpha u-\beta uv\end{bmatrix}\\&\quad+\begin{bmatrix}-8uv\\ 3v^2-3c^2+(1-b)w^2-4u^2\\ 2(1-b)vw\end{bmatrix},\end{aligned}$$

(IV) the financial chaotic system:[31]

$$\begin{bmatrix}\dot{x}_1\\ \dot{x}_2\\ \dot{x}_3\end{bmatrix}=\begin{bmatrix}x_3+(x_2-a)x_1\\ 1-bx_2-x_1^2\\ -x_1-cx_3\end{bmatrix}=\begin{bmatrix}x_3\\ 1-x_1^2-\frac{1}{2}x_1^2\\ -x_1\end{bmatrix}+\begin{bmatrix}(x_2-a)x_1\\ -bx_2+\frac{1}{2}x_1^2\\ -cx_3\end{bmatrix},$$

(V) the dynamical system without equilibrium points:[16]

$$\begin{bmatrix}\dot{x}\\ \dot{y}\\ \dot{z}\end{bmatrix}=\begin{bmatrix}y^2-x+zy\\ x-xz+a+zy\\ zx-a-y\end{bmatrix}=\begin{bmatrix}y^2+zy-\frac{1}{2}z^2\\ x-xz+a\\ -a-y-\frac{1}{2}y^2\end{bmatrix}+\begin{bmatrix}-x+\frac{1}{2}z^2\\ zy\\ zx+\frac{1}{2}y^2\end{bmatrix},$$

(VI) the Sprott D system:[32]

$$\begin{bmatrix}\dot{x}\\ \dot{y}\\ \dot{z}\end{bmatrix}=\begin{bmatrix}-y\\ x+z\\ xz+3y^2\end{bmatrix}=\begin{bmatrix}-y-\frac{1}{2}z^2\\ x+z\\ 3y^2\end{bmatrix}+\begin{bmatrix}\frac{1}{2}z^2\\ 0\\ xz\end{bmatrix}.$$

Step 2: Solving the Hamilton energy function Before introducing the specific solution, we need to elaborate on the concept of generalized Hamilton systems. In the state space $X=(x_1,x_2,x_3,\ldots,x_n)^{\mathrm{T}}\in\mathbb{R}^n$, generalized Hamilton systems can be described by

$$\dot{X}=M(X)\nabla H+g(X)u(X,t), \tag{8}$$

where $H(X)$ is the Hamilton energy, $\nabla H=(\partial H(x)/\partial x_1,\partial H(x)/\partial x_2,\ldots,\partial H(x)/\partial x_n)^{\mathrm{T}}$ is the gradient vector of the smooth energy function, and $g(X,t)$ is the input vector, the $g(X,t)$ is time-independent input. A generalized Hamilton system can be decomposed into two symmetric matrices $R(X)$ and $S(X)$, and one anti-symmetric matrix $J(X)$. The sum of $R(X)$ and $S(X)$ is also called the dissipative matrix. Thus, Eq. (8) can be rewritten as

$$\dot{X}=[J(X)-R(X)+S(X)]\nabla H(X)+g(X)u(X,t), \tag{9}$$

where $J(X)$ denotes the conservative part of energy, $R(X)$ denotes the system's energy dissipation, $S(X)$ denotes the produced within the system, and $g(X)u(X,t)$ denotes the input of external energy. We make

$$\begin{aligned}f_{\mathrm{c}}(X)&=J(X)\nabla H(X),\\ f_{\mathrm{d}}(X)&=[-R(X)+S(X)]\nabla H(X).\end{aligned} \tag{10}$$

The system can be rewritten as

$$\dot{X}=f_{\mathrm{c}}(X)+f_{\mathrm{d}}(X)+g(X)u(X,t), \tag{11}$$

$$M(X)\nabla H=f_{\mathrm{c}}(X)+f_{\mathrm{d}}(X). \tag{12}$$

The terms $f_{\mathrm{c}}(X)$ and $f_{\mathrm{d}}(X)$ satisfy the following equations:

$$\nabla H^{\mathrm{T}}(X)f_{\mathrm{c}}(X)=0, \tag{13}$$

$$\nabla H^{\mathrm{T}}(X)f_{\mathrm{d}}(X)=\frac{\mathrm{d}H(X)}{\mathrm{d}t}. \tag{14}$$

The simple proof of Eq. (13) can be found in previous studies.[17] Since $J(X)$ is an anti-symmetric matrix, that is, $J(X)=-J(X)$, it is easy to get $\nabla H^{\mathrm{T}}(X)J(X)H(X)=0$. Putting $f_{\mathrm{c}}(X)=J(X)\nabla H(X)$ into $\nabla H^{\mathrm{T}}(X)J(X)H(X)=0$ can get $\nabla H^{\mathrm{T}}(X)f_{\mathrm{c}}(X)=0$.

Table 1. Vector fields directly decomposed (type I) and decomposed by exterior differentiation (type II).

Type I		Type II	
Name	Model	Name	Model
Lorenz system	$\begin{cases}\dot{x}=\sigma y-\sigma x,\\ \dot{y}=\rho x-y-xz,\\ \dot{z}=xy-\beta z.\end{cases}$	Rössler system	$\begin{cases}\dot{x}=-y-z,\\ \dot{y}=x+ay,\\ \dot{z}=b+(x-c)z.\end{cases}$
Chua system	$\begin{cases}\dot{x}=\alpha y-\alpha x^3-\alpha cx,\\ \dot{y}=x+z-y,\\ \dot{z}=-\beta y.\end{cases}$	the equations of motion of the unconstrained particle	$\begin{cases}\dot{x}=x_1,\\ \dot{x}_1=ax-bx^2-cx_1y,\\ \dot{y}=y_1,\\ \dot{y}_1=ay-by^2-cxy_1.\end{cases}$
Chen system	$\begin{cases}\dot{x}=ay-ax,\\ \dot{y}=(c-a)x+cy-xz,\\ \dot{z}=xy-bz.\end{cases}$	four-wing chaotic system	$\begin{cases}\dot{u}=\alpha w-8uv,\\ \dot{v}=11u^2+3v^2+w^2+\beta uw-3c^2,\\ \dot{w}=-\alpha u+2(1-b)vw-\beta uv.\end{cases}$
Lü system	$\begin{cases}\dot{x}=ay-ax,\\ \dot{y}=cy-xz,\\ \dot{z}=xy-bz.\end{cases}$	dynamical system without equilibrium points	$\begin{cases}\dot{x}=y^2-x+zy,\\ \dot{y}=x-xz+a+zy,\\ \dot{z}=zx-a-y.\end{cases}$
HR system	$\begin{cases}\dot{x}=y-ax^3+bx^2+I-z,\\ \dot{y}=c-dx^2-y,\\ \dot{z}=r[s(x-x_0)-z].\end{cases}$	financial chaotic system	$\begin{cases}\dot{x}_1=x_3+(x_2-a)x_1,\\ \dot{x}_2=1-bx_2-x_1^2,\\ \dot{x}_3=-x_1-cx_3.\end{cases}$
4D HR system	$\begin{cases}\dot{x}=ay+bx^2-cx^3-dz+\xi I,\\ \dot{y}=e-fx^2-y-gw,\\ \dot{z}=m[-z+s(x+h)],\\ \dot{w}=n[-kw+r(y+l)].\end{cases}$	Sprott D system	$\begin{cases}\dot{x}=-y,\\ \dot{y}=x+z,\\ \dot{z}=xz+3y^2.\end{cases}$

Due to the fact that most physical systems have energy storage, consumption, and production, as well as external energy input, it is easy to understand the energy changes within the system if we put the system into a generalized Hamilton form. According to the definition,[17] the conditions, under which affine nonlinear dynamical systems can be converted to generalized Hamilton systems, are such that $F(X)$ can be decomposed to $f_{\mathrm{c}}(X)+f_{\mathrm{d}}(X)$. Finding the system's energy func-

tion (usually unknown) is crucial for obtaining this form. It can be achieved by solving the first-order linear homogeneous partial differential equation, which is inferred by Eq. (13). Here we introduce a method to solve this type of partial differential equation (PDE): the characteristic curve method. The key to this method is to convert PDE into a set of ordinary differential equations (ODEs) to solve. We can derive the characteristic equations related to PDE based on the characteristic lines and solve the ordinary differential equations through the first integral. We can get a first-order partial differential equation from Eq. (13):

$$\sum_{i=1}^{n} a_i(x_1, x_2, \ldots, x_n)\frac{\partial u}{\partial x_i} = 0, \tag{15}$$

where a_i is a known function of the corresponding variable, it is continuously differentiable in the region $\Omega \in \mathbb{R}^n$ and the partial derivatives with respect to each independent variable x_i are bounded.

Before elaborating on the characteristic curve method for solving first-order linear homogeneous partial differential equations, it is necessary to introduce its geometrical significance in three dimensions. Given a direction field $\boldsymbol{F} = [P(x,y,z)\boldsymbol{i}, Q(x,y,z)\boldsymbol{j}, R(x,y,z)\boldsymbol{k}]$, where P, Q, R are continuous functions of x, y, z, and $\boldsymbol{i}, \boldsymbol{j}, \boldsymbol{k}$ are unit vectors. If a curve in space has a tangent vector at every point, and the direction of the tangent vector is the same as the direction of the vector field $\boldsymbol{F}$, then such a curve is called a characteristic curve. According to this character, we can get a symmetric form

$$\frac{\mathrm{d}x}{P(x,y,z)} = \frac{\mathrm{d}y}{Q(x,y,z)} = \frac{\mathrm{d}z}{R(x,y,z)}. \tag{16}$$

The characteristic surface of the vector field $\boldsymbol{F}$ means that the normal vector $\boldsymbol{N}$ of the surface is orthogonal to the direction of the vector field $\boldsymbol{F}$ at any point. Suppose that the equation of the characteristic surface is $u(x,y,z) = C$ (C is a constant), then its normal vector is $\boldsymbol{N} = (\frac{\partial u}{\partial x}\boldsymbol{i}, \frac{\partial u}{\partial y}\boldsymbol{j}, \frac{\partial u}{\partial z}\boldsymbol{k})$. According to the vertical relationship, we can obtain the equation

$$\begin{aligned}\boldsymbol{N}\cdot\boldsymbol{F} &= \left(\frac{\partial u}{\partial x}\boldsymbol{i}, \frac{\partial u}{\partial y}\boldsymbol{j}, \frac{\partial u}{\partial z}\boldsymbol{k}\right)\cdot[P(x,y,z)\boldsymbol{i}, Q(x,y,z)\boldsymbol{j}, R(x,y,z)\boldsymbol{k}] \\ &= 0.\end{aligned} \tag{17}$$

That is to say, the left-hand side of the equation is essentially the directional derivative of u in the direction of vector field $\boldsymbol{F}$. Equation (16) is a characteristic of Eq. (17), and the solutions of Eq. (16) signify the characteristic curve. Therefore, the problem of geometrically solving characteristic surfaces is transformed into the problem of solving PDE.

The characteristic curve method is a widely used approach for solving first-order homogeneous linear partial differential equation. For Eq. (15), its characteristic equations can be written as

$$\frac{\mathrm{d}x_1}{a_1(x_1, x_2, \ldots, x_n)} = \frac{\mathrm{d}x_2}{a_2(x_1, x_2, \ldots, x_n)} = \cdots = \frac{\mathrm{d}x_n}{a_n(x_1, x_2, \ldots, x_n)}. \tag{18}$$

According to this set of ODEs, the $n-1$ first integrals can be solved, and the Hamilton energy function is usually a combination of these first integrals.

Step 3: Verifying uniqueness According to the previous steps, we can obtain an infinite solution of ODEs. The uniqueness of the Hamilton energy function still needs to be tested, specifically to verify Eq. (14). The solution that satisfies uniqueness is the appropriate energy function,

$$\frac{\mathrm{d}H(X)}{\mathrm{d}t} = \nabla H^{\mathrm{T}}(X)\dot{X} = \nabla H^{\mathrm{T}}(X) f_{\mathrm{d}}(X). \tag{19}$$

3. Numerical simulations

In this section, numerical simulations for the five systems mentioned above are carried out by using the fourth-order Runge–Kutta algorithm with time steps of $h = 0.01$, transient period about 30 time units. The initial values are selected to be $(-1.6, 0.5, 21)$ for Lorenz system, (0, 1, 0) for Chen system, (5, −5, 5) for Lü system, and $(-1.6, -0.5, 2)$ for Rössler system. In order to investigate the energy evolution of Rössler system more comprehensively, the transient period was sat as 300 time units. The simulation results are shown in Fig. 1.

In particular, the HR and 4D HR systems mentioned above are discussed in more detail here. The variables x, y, and z in the HR system represent the membrane potential, slow current, and the recovery variable of adaptive current, respectively. The remaining parameters are set as $a = 1$, $b = 3$, $c = 1$, $d = 5$, $s = 4$, and $r = 0.006$. Because the electrophysiological environment of real neurons is very complex, the variable w describing slow calcium current is added to the 4D HR neuron model in order to further analyze the dynamic behavior of neurons. The remaining parameters are set as $a = 1$, $b = 3$, $c = 1$, $d = 0.99$, $\xi = 1$, $e = 1.01$, $f = 5.0128$, $g = 0.0278$, $m = 0.00215$, $s = 3.966$, $h = 1.605$, $n = 0.0009$, $k = 0.9573$, $r = 3.0$, and $l = 1.619$. The initial values are selected to be (1, −2, −2) and (0.5, 1, 2, 2), and the transient periods are sat as 3000 time units.

Due to the complexity of the electrophysiological environment in which genuine neurons exist, even minor alterations in external circumstances can result in neurons displaying entirely distinct electrical activity patterns. This manuscript applies periodic signals with both high and low frequencies to the neuron model in an attempt to better mimic the brain environment of real neurons. Apart from this stimulation mode, it is also possible to investigate how noise and other variables affect the neuron model's firing style. The change of membrane potential under the external forcing current $I_{\mathrm{ext}} = I + A\cos\omega t + B\cos(N\omega t + \varphi)$ is shown in Figs. 2 and 3, where I is a constant current, A and B represent the

amplitude and ω represents the angular frequency of the periodic forcing current, respectively.[33] It can be seen that both systems exhibit regular spikes and cluster discharges when the parameters of external signals are set appropriately. It can also be found that the change trend of Hamilton energy function is opposite to that of membrane potential, which may be related to the energy consumption required for the generation of neuron action potential. Furthermore, the interspike interval (ISI) of HR system membrane potential under the change of the angular frequency ω and amplitude A is shown in Fig. 4, and the ISI of 4D HR system membrane potential under the change of the angular frequency ω and amplitude B is shown in Fig. 5. It can be seen from the ISI diagram that both the HR system and the 4D HR system exhibit rich discharge modes with the change of external signal parameters.

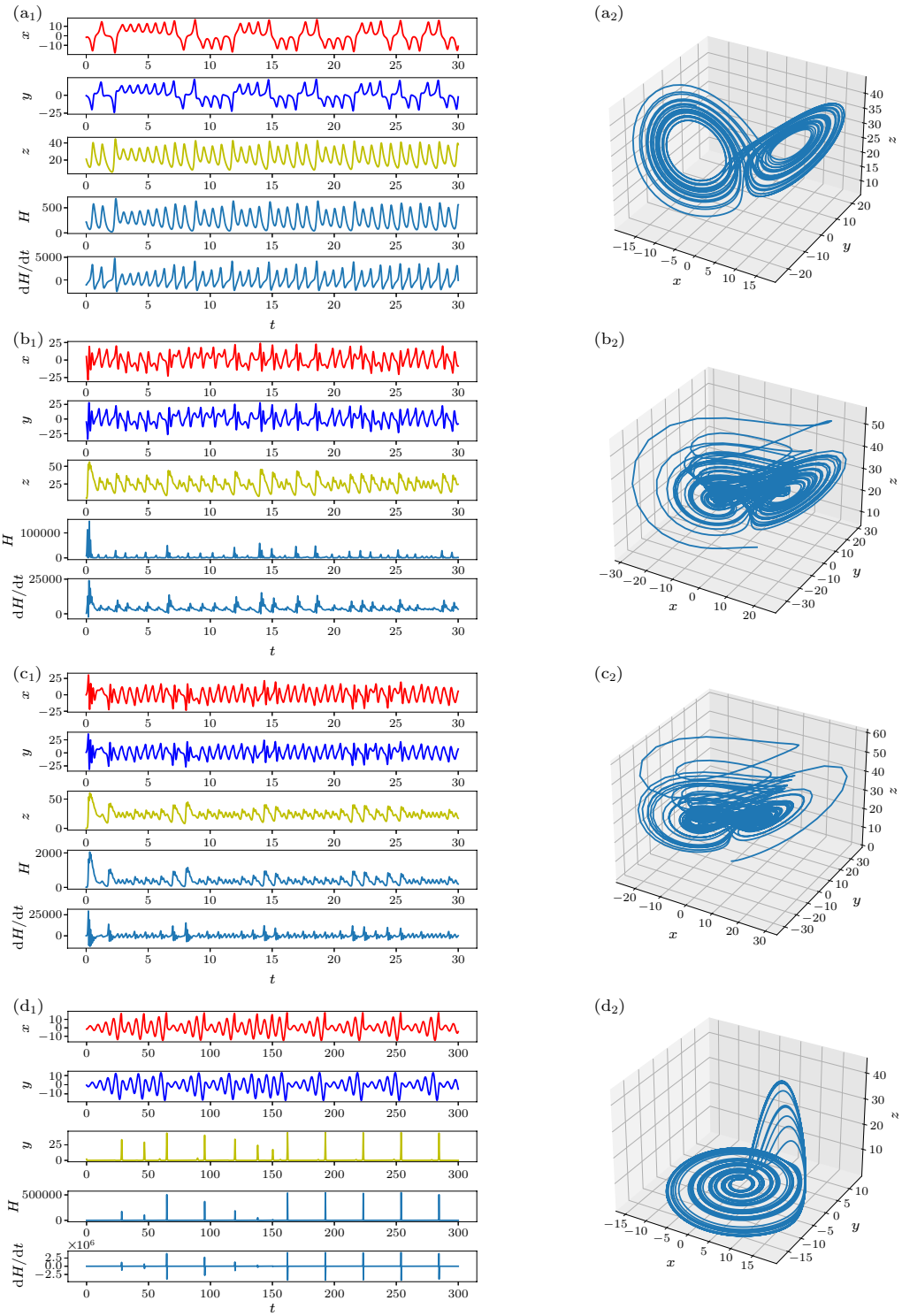


Fig. 1. Lorenz system (a), Lü system (b), Chen system (c), and Rössler system (d). [(a_1), (b_1), (c_1), (d_1)] Sample time series of state variables and development of Hamilton energy. [(a_2), (b_2), (c_2), (d_2)] Phase portraits.

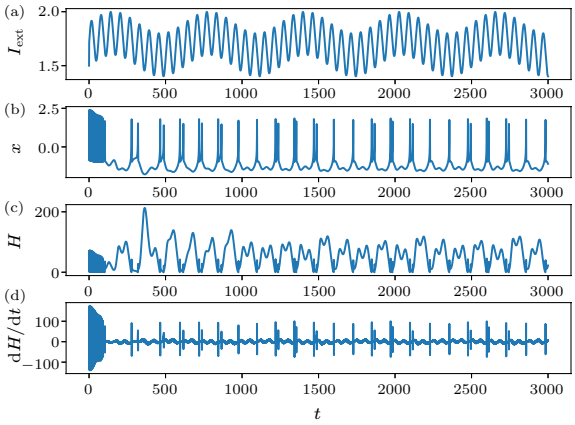


Fig. 2. HR system: (a) sample time series of cosine signal; (b) sample time series of membrane potential; (c) the development of Hamilton energy; (d) the change of Hamilton energy versus time.

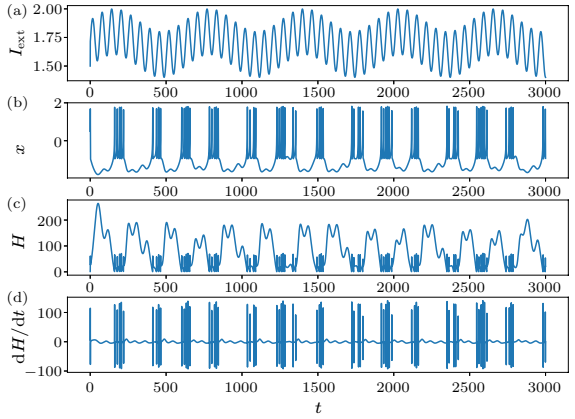


Fig. 3. Four-dimensional HR system: (a) sample time series of cosine signal; (b) sample time series of membrane potential; (c) the development of Hamilton energy; (d) the change of Hamilton energy versus time.

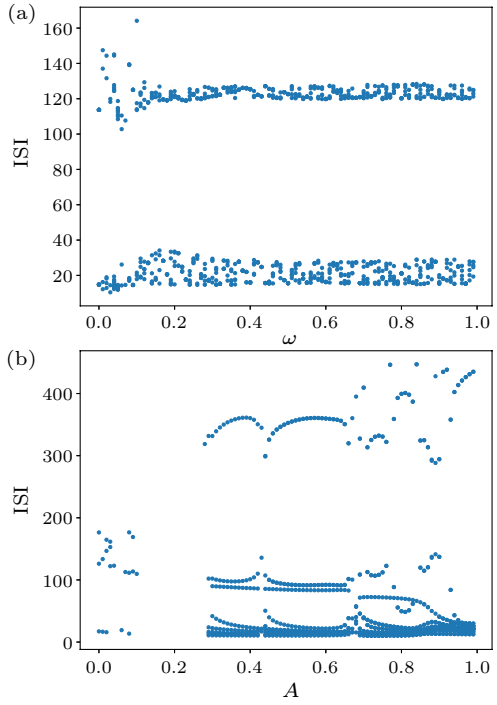


Fig. 4. The ISI bifurcation diagram of HR system: (a) ISI versus ω for $A = 0.1$, $B = 0.2$, $N = 100$. The pulse interval of the neuron with the increase of ω is around 20 and 120. (b) ISI versus A for $\omega = 0.01$, $B = 0.2$, $N = 1$. The pulse interval of neuron is more regular when the middle value of A is taken.

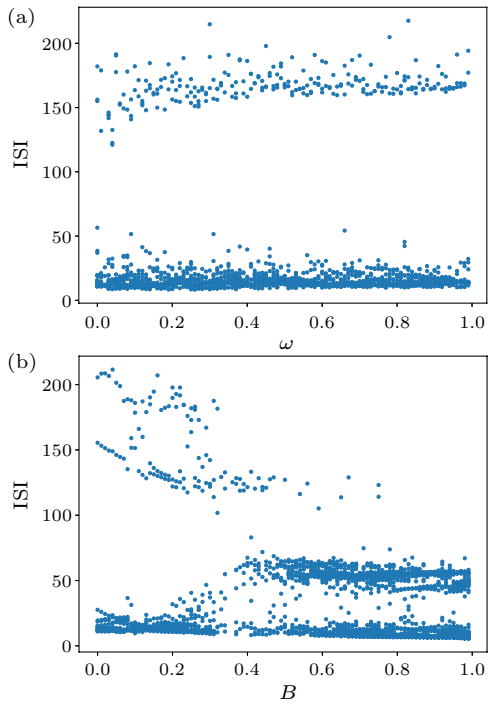


Fig. 5. The ISI bifurcation diagram of 4D HR system: (a) ISI versus ω for $A = 0.1$, $B = 0.2$, $N = 10$. The pulse interval of the neuron with the increase of ω is around 20 and 160. (b) ISI versus B for $\omega = 0.01$, $A = 0.1$, $N = 10$. The pulse interval of neuron is more regular when the large value of B is taken.

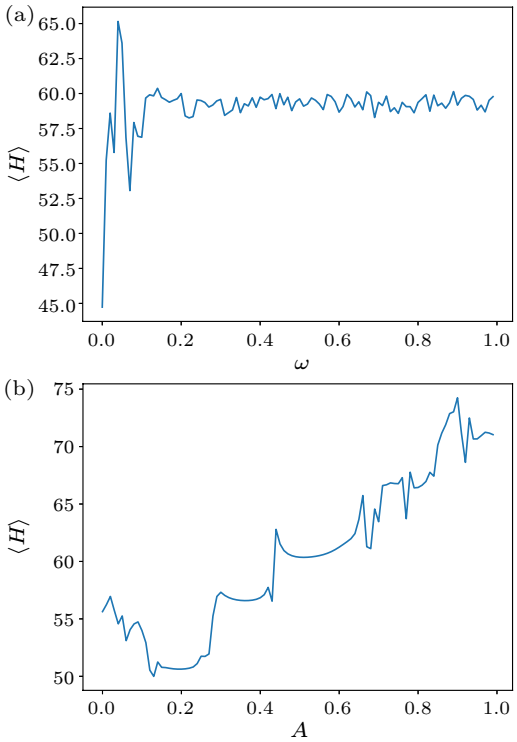


Fig. 6. (a) Dependence of average energy $\langle H \rangle$ of HR system on frequency ω for $A = 0.1$, $B = 0.2$, $N = 100$. The average energy of the system is greatly affected when ω is small. (b) Dependence of average energy $\langle H \rangle$ of HR system on amplitude A for $B = 0.2$, $\omega = 0.01$, $N = 1$. The average energy of the system shows an increasing trend with the increase of A.

The dependence of average energy $\langle H \rangle$ of the HR system on amplitude A and frequency ω is shown in Fig. 6, and the dependence of average energy $\langle H \rangle$ of the 4D HR system on

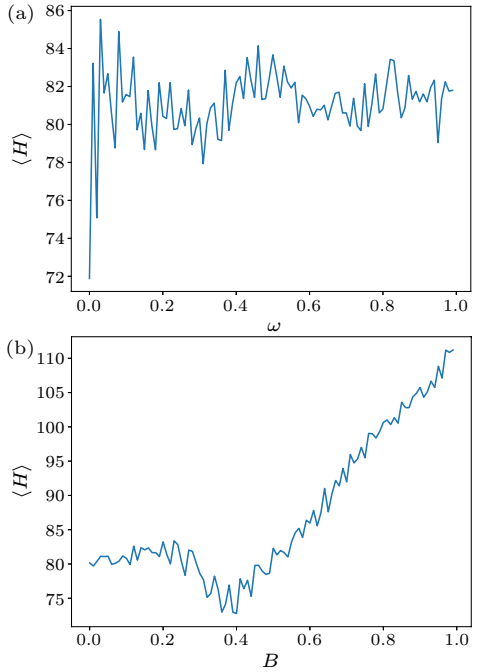


Fig. 7. (a) Dependence of average energy $\langle H\rangle$ of 4D HR system on frequency ω for $A = 0.1$, $B = 0.2$, $N = 10$. The average energy of the system is greatly affected when ω is small. (b) Dependence of average energy $\langle H\rangle$ of 4D HR system on amplitude B for $A = 0.1$, $\omega = 0.01$, $N = 10$. The average energy of the system decreases first and then increases with the increase of B.

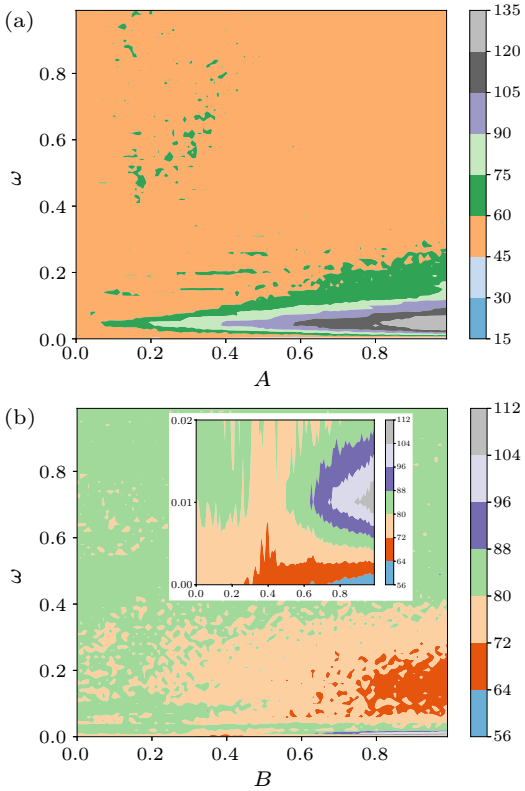


Fig. 8. (a) Synergistic effects of angular frequency ω and amplitude A on the average energy $\langle H\rangle$ in HR system for $B = 0.2$, $N = 100$. (b) Synergistic effects of angular frequency ω and amplitude B on the average energy $\langle H\rangle$ in 4D HR system for $A = 0.1$, $N = 10$.

amplitude B and frequency ω is shown in Fig. 7. It can be observed that the amplitude of an external signal has a greater effect on the average energy of neurons than the angular frequency. In addition, an interesting phenomenon can be observed in Fig. 7(b). As the amplitude B increases, the average energy of neurons first decreases and then increases, and there is a minimum value within the range of parameter values. Finally, the synergistic effect of angular frequency and amplitude on the average energy $\langle H\rangle$ is also shown in Fig. 8. It can be found that the average energy of neurons can be kept low by proper parameter settings in Fig. 8(b), which is consistent with Fig. 7.

4. Discussion and conclusion

In previous research about dynamical systems, Hamilton energy, as an important quantitative analysis tool, has been widely used in processes of dynamical behavior analyses. The steps to derive the energy function may not be same for different systems, so it is necessary to find the common rules that different systems follow in the derivation processes.

Based on the Helmholtz theorem, a solution method was proposed to deduce the system's Hamilton energy function. We have summarized the three steps of this method, that is, step 1, decomposing the vector field; step 2, solving the Hamilton energy function according to the equation; and step 3, verifying uniqueness, respectively. In the step of decomposing vector fields, two different decomposition ideas were proposed based on the form of state variables. Then, we drew a table to illustrate some classical systems and divided them into types I and Ⅱ under the different decomposition methods. For example, the Lorenz system, the Chua system, etc. that can be decomposed directly belong to type I. In addition, some systems, such as the Rössler system, simplified financial chaotic system, chaotic system with hidden attractors, etc., need to be matched by exterior differentiation before decomposing belong to type Ⅱ. In this way, we can ensure $\mathrm{div} f_{\mathrm{c}}(X) = 0$ and $\mathrm{rot} f_{\mathrm{d}}(X) = 0$. In the step of solving the energy function according to the equation, a set of ODEs related to the first-order partial differential equation is obtained by the characteristic line method. For the obtained set of ODEs, the energy function can be solved using the first integral or the matching method based on the ratio theorem. Finally, we need to verify the uniqueness of the energy function. At the end of this manuscript, the Hamilton energy evolution of six classical systems is shown.

In summary, this contribution proposes a common method to deduce the Hamilton energy function that can be used as a measurement instrument to estimate the cost to a system of generating dynamic behaviors. Memristive systems are an important component of nonlinear systems, and previous work has investigated memristive systems from an energy perspective.[20,34–38] It is expected that the energy function of the memristive system will be determined using this solution method. This method also provides some ideas for choosing

decomposition methods and dealing with high-dimensional systems. We hope it can inspire scholars to study nonlinear dynamics.

Acknowledgment

This work was supported by the National Natural Science Foundation of China (Grant Nos. 12305054, 12172340, and 12371506)

References

[1] Lu L L, Jia Y, Xu Y, Ge M Y, Yang L J and Zhan X 2018 *Sci. China Technol. Sci.* **62** 427
[2] Yang Y M, Ma J, Xu Y and Jia Y 2020 *Cogn. Neurodyn.* **15** 265
[3] Lin H R, Wang C H, Yao W and Tan Y M 2020 *Commun. Nonlinear Sci. Numer. Simulat.* **90** 105390
[4] He Z W and Yao C G 2020 *Sci. China Technol. Sci.* **63** 2339
[5] Lu L L, Gao Z H, Wei Z C and Yi M 2023 *Chaos* **33** 013127
[6] Yang F F, Wang Y and Ma J 2023 *Commun. Nonlinear Sci. Numer. Simulat.* **119** 107127
[7] Torrealdea F J, d'Anjou A, Graña M and Sarasola C 2006 *Phys. Rev. E* **74** 011905
[8] Yao C G, Yao Y G, Qian Y and Xu X F 2022 *Chaos, Solitons Fractals* **164** 112667
[9] Xu Y and Ma J 2022 *Commun. Nonlinear Sci. Numer. Simulat.* **111** 106426
[10] Lu L L, Yi M, Gao Z H, Wu Y and Zhao X 2023 *Nonlinear Dyn.* **111** 16557
[11] Torrealdea F J, Sarasola C and d'Anjou A 2009 *Chaos, Solitons Fractals* **40** 60
[12] Lv M, Ma J, Yao Y G and Alzahrani F 2018 *Sci. China Technol. Sci.* **62** 448
[13] Wang G W, Xu Y, Ge M Y, Lu L L and Jia Y 2020 *AEU Int. J. Electron. Commun.* **120** 153209
[14] Song X L, Jin W Y and Ma J 2015 *Chin. Phys. B* **24** 128710
[15] Sarasola C, D'Anjou A, Torrealdea F J and Moujahid A 2005 *Int. J. Bifur. Chaos* **15** 2507
[16] Ma J, Wu F Q, Jin W Y, Zhou P and Hayat T 2017 *Chaos* **27** 053108
[17] Cang S J, Wu A G, Wang Z H and Chen Z Q 2017 *Int. J. Bifur. Chaos* **27** 1750024
[18] Huang L L, Ma Y H and Li C 2024 *Chin. Phys. B* **33** 010503
[19] Guo Y L, Qi G Y and Hamam Y 2016 *Nonlinear Dyn.* **85** 2765
[20] Yamakou M E 2020 *Nonlinear Dyn.* **101** 487
[21] Ortigueira M D, Rivero M and Trujillo J J 2015 *Commun. Nonlinear Sci. Numer. Simulat.* **22** 1036
[22] Sarasola C, Torrealdea F J, d'Anjou A, Moujahid A and Graña M 2004 *Phys. Rev. E* **69** 011606
[23] An X L and Zhang L 2018 *Nonlinear Dyn.* **94** 2995
[24] Aqeel M, Azam A and Ahmad S 2018 *Chin. J. Phys.* **56** 1220
[25] Yao Z, Zhou P, Alsaedi A and Ma J 2020 *Appl. Math. Comput.* **374** 124998
[26] Azam A, Aqeel M and Hussain Z 2020 *Soft Comput.* **25** 2521
[27] Ezhilarasu P M, Inbavalli M, Murali K and Thamilmaran K 2018 *Pramana* **91** 4
[28] Njitacke Z T, Koumetio B N, Ramakrishnan B, Leutcho G D, Fozin T F, Tsafack N, Rajagopal K and Kengne J 2021 *Cogn. Neurodyn.* **16** 899
[29] Li J H, Wu H B and Mei F X 2017 *Nonlinear Dyn.* **90** 2557
[30] Azam A, Aqeel M, Ahmad S and Ahmad F 2017 *Nonlinear Dyn.* **90** 1
[31] Tirandaz H, Aminabadi S S and Tavakoli H 2018 *Alexandria Eng. J.* **57** 1519
[32] Sprott J C 1994 *Phys. Rev. E* **50** R647
[33] Torrealdea F J, Sarasola C, d'Anjou A, Moujahid A and de Mendizábal N V 2009 *Biosystems* **97** 60
[34] Bao H, Yu X H, Zhang Y Z, Liu X F and Chen M 2023 *Chaos, Solitons Fractals* **177** 114167
[35] Njitacke Z T, Takembo C N, Awrejcewicz J, Fouda H P E and Kengne J 2022 *Chaos, Solitons Fractals* **160** 112211
[36] Thottil S K and Ignatius R P 2018 *Nonlinear Dyn.* **95** 239
[37] Wang C N, Sun G P, Yang F F and Ma J 2022 *AEU Int. J. Electron. Commun.* **153** 154280
[38] Xu L, Qi G Y and Ma J 2022 *Appl. Math. Model.* **101** 503